Neuron, Vol. 16, 345–355, February, 1996, Copyright ©1996 by Cell Press

Requirement for Superoxide in Excitotoxic Cell Death

Manisha Patel,* Brian J. Day,* James D. Crapo,* Irwin Fridovich,† and James O. McNamara*‡§‖
*Department of Medicine
†Department of Biochemistry
‡Department of Neurobiology
§Department of Pharmacology
Duke University
Durham, North Carolina 27710
‖Veteran's Administration Medical Center
Durham, North Carolina 27710

Summary

We tested the pathogenic role of O_2^- radicals in excitotoxic injury. Inactivation of the TCA cycle enzyme, aconitase, was used as a marker of intracellular O_2^- levels, and a porphyrin SOD mimetic was used to scavenge O_2^-. The selective, reversible, and SOD-sensitive inactivation of aconitase by known O_2^- generators was used to validate aconitase activity as a marker of O_2^- generation. Treatment of rat cortical cultures with NMDA, KA, or the intracellular O_2^- generator PQ^{2+} produced a selective and reversible inactivation of aconitase, which closely correlated with subsequent cell death produced by these agents. The SOD mimetic, but not its less active congener, attenuated both aconitase inactivation and cell death produced by NMDA, KA, and PQ^{2+}. These results provide direct evidence implicating O_2^- generation in the pathway to excitotoxic injury.

Introduction

Cell death in diverse neurological disorders may occur in part from excessive activation of glutamate receptors, resulting in excitotoxic damage (Olney, 1986, 1989; Choi, 1988). Excitotoxic death requires the influx of extracellular Ca^{2+} via receptor-operated channels or voltage-sensitive Ca^{2+} channels (Choi, 1985; Garthwaite and Garthwaite, 1986); the excessive intracellular Ca^{2+} (Ca^{2+}_i) initiates a series of molecular events that culminate in neuronal death (Choi, 1988). Although the initial steps in the excitotoxic process, such as the requirement for Ca^{2+} influx, are known, the molecular events by which a rise in Ca^{2+}_i triggers death of neurons are largely unknown.

Several lines of recent evidence suggest that reactive oxygen species (ROS), particularly superoxide (O_2^-) radicals, play a pivotal role in the pathogenesis of excitotoxic death (for review, see Coyle and Puttfarcken, 1993). First, transgenic mice that overexpress the cytoplasmic copper, zinc superoxide dismutase (CuZnSOD) are resistant to ischemic brain damage (Kinouchi et al., 1991), a form of damage mediated in part by glutamate receptor activation. Neurons derived from these transgenic mice are resistant to glutamate toxicity in vitro (Chan et al., 1990). Second, the putative lipid peroxidation inhibitors, 21-aminosteroids, can partly attenuate excitotoxic damage in vitro (Monyer et al., 1990; Puttfarcken et al., 1993), suggesting that free radical–mediated lipid peroxidation may be a downstream event in the excitotoxic process. Third, using electron paramagnetic resonance (EPR) coupled with spin trap agents, Lafon-Cazal et al. (1993) provide direct evidence that N-methyl-D-aspartate (NMDA) can generate O_2^- radicals in the extracellular space, and they demonstrate neuroprotective effects of the spin trap agents against NMDA toxicity. By contrast, kainate (KA) toxicity was not associated with generation of O_2^- radicals.

A more definitive role for ROS has emerged in the pathogenesis of programmed cell death (PCD) based on studies demonstrating: antioxidant action of the anti-apoptotic protein, Bcl2 (Hockenbery et al., 1993; Kane et al., 1993); protection by SOD against PCD (Greenlund et al., 1995; Jordan et al., 1995); and the induction of PCD by down-regulation of SOD (Rothstein et al., 1994; Troy and Shelanski, 1994). The most notable pathogenic role for ROS has emerged from the identification of mutations in the gene encoding CuZnSOD from individuals with familial amyotrophic lateral sclerosis (Rosen et al., 1993), a mutation that results in the conversion of SOD from an anti-apoptotic gene to a pro-apoptotic gene (Rabizadeh et al., 1995).

One straightforward approach to test the idea that O_2^- radicals mediate excitotoxic neuronal death would be to use CuZnSOD, which metabolizes O_2^- radicals (McCord and Fridovich, 1969), to block excitotoxic cell death. However, attempts to protect neurons from excitotoxic death with the use of purified CuZnSOD have been largely unsuccessful, presumably because of the large, membrane-impermeable nature of this enzyme (Lafon-Cazal et al., 1993; M. P. and J. O. M., unpublished data).

In light of the evidence suggesting a role for O_2^- in cell death, a cell-permeable mimetic of SOD can be a useful tool to probe the mechanism of cell death and may be beneficial as a pharmacological agent to ameliorate cell death in a variety of conditions. The Mn(III) porphyrin 5,10,15,20-tetrakis(benzoic acid) porphyrin manganese(III) (MnTBAP) belongs to a unique category of SOD mimetics that satisfy the criteria required for an ideal mimetic: it is active, stable, and nontoxic, much like SOD itself (Faulkner et al., 1994). The Mn(III) moiety of the SOD mimetic can function in the dismutation reaction with O_2^- by undergoing alternate reduction and oxidation. Manganic SOD mimetics have a high rate of reaction with O_2^- (k_T) in a cell-free system ($k_T = 6 \times 10^6$ $M^{-1}s^{-1}$; Day et al., 1995) and probably higher rates within the intracellular environment ($k_T = 2 \times 10^9$ $M^{-1}s^{-1}$; Liochev and Fridovich, 1995). The latter is presumably achieved by the action of cellular reductants that keep the manganese in its reduced state. Thus, the Mn(III) porphyrins are much like the cell's own SOD in their rate of reaction with O_2^- ($k_T = 2 \times 10^9$ $M^{-1}s^{-1}$ of Mn(II) porphyrins in vivo versus $k_T = 3 \times 10^9$ $M^{-1}s^{-1}$ of CuZnSOD). Unlike SOD, the Mn(III) porphyrins have the advantage of being able to penetrate cellular membranes (Day et al., 1995). These attributes contribute to the ability of several of these compounds to protect Escherichia coli

from oxidative stress (Faulkner et al., 1994; Liochev and Fridovich, 1995). MnTBAP has also been found to protect mammalian cells against oxidative damage (Day et al., 1995).

A sensitive and specific intracellular marker for O_2^- detection is highly desirable. A physiological intracellular target sensitive to modification by O_2^- could be used as an indicator of O_2^- concentrations. One such intracellular target described in E. coli is the tricarboxylic acid (TCA) cycle enzyme, aconitase. The iron–sulfur (Fe–S) center of E. coli aconitase can be reversibly inactivated by O_2^- and its reaction product peroxynitrite (Gardner and Fridovich, 1992; Hausladen and Fridovich, 1994), allowing the measurement of aconitase activity to serve as an indicator of O_2^- production. Recently, progress has been made in the development of aconitase as an intracellular indicator of O_2^- and peroxynitrite in E. coli (Gardner and Fridovich, 1991, 1992; Hausladen and Fridovich, 1994) and mammalian cells (Gardner et al., 1995). Two properties of aconitase make it an attractive marker for O_2^- detection in the cell. First, the action of O_2^- converts the active $[4Fe–4S]^{2+}$-containing form of aconitase to the inactive $[3Fe–4S]^{+}$-containing form (equation 1), allowing a change in its activity to be used as a marker of O_2^-. Second, as shown in equation 2, the inactive aconitase can be repaired by the insertion of iron in the presence of intracellular sulfhydryls such as reduced glutathione (GSH), restoring the active form and confirming the mechanism of its inactivation. It is this inactivation and reactivation of aconitase that constitutes the normal dynamic state. Mammalian aconitase closely resembles its E. coli counterpart in that it has an Fe–S center (Flint et al., 1993) that can be reversibly activated (Kennedy et al., 1983).

$$[4Fe–4S]^{2+}_{active} + O_2^- + 2H^+ \rightarrow [3Fe–4S]^{+}_{inactive} + Fe^{2+} + H_2O_2 \quad (1)$$

$$[3Fe–4S]^{+}_{inactive} + Fe^{2+} + GSH \rightarrow [4Fe–4S]^{2+}_{active} + 1/2GSSG + H^+ \quad (2)$$

Using aconitase activity as an intracellular marker of O_2^- generation, together with a cell-permeant SOD mimetic, we investigated the role of O_2^- generation in excitotoxic cell death. Specifically, we sought to address the following questions. Is aconitase activity a valid marker of O_2^- radical formation in cortical cell culture? Do toxic concentrations of NMDA and KA produce selective and reversible inactivation of aconitase, and if so, does this correlate with subsequent neuronal death? Can a SOD mimetic prevent aconitase inactivation and cell death produced by O_2^- generators, NMDA, and KA?

Results

Validation of Aconitase Activity as a Marker of O_2^- Radical Formation in Cortical Cell Culture

With the use of agents that are known to generate O_2^- (xanthine plus xanthine oxidase [X+XO] and paraquat [PQ^{2+}]), we considered four criteria necessary to establish the validity of aconitase activity as a marker of O_2^-. O_2^- generators were tested for their ability to inactivate aconitase, to do so in a SOD-preventable manner, to inactivate aconitase selectively in comparison to another TCA cycle enzyme, and to inactivate aconitase reversibly, thereby providing insight into the mechanism of the inactivation process. That is, reversibility by iron and a reducing agent would imply that inactivation was mediated by a posttranslational mechanism involving the Fe–S center of aconitase.

We first examined the effects of known O_2^--generating compounds on aconitase activity in cortical cells. X+XO and PQ^{2+} are known to generate O_2^- (Fridovich, 1970; Bus and Gibson, 1984) and were used to examine these criteria. The X+XO system can generate O_2^- radicals by the oxidation of xanthine by xanthine oxidase. The X+XO system generates O_2^- radicals in the extracellular environment. Since O_2^- generated extracellularly by the incubation of cells with X+XO does not have access to its target, the intracellular aconitase, X+XO was added directly to cell lysates prepared from untreated cortical cultures, and aconitase activity was measured in these lysates. To rule out a role of peroxide in aconitase inactivation, catalase was included while testing the effects of X+XO. Aconitase activity was decreased by treatment of cell lysates for 30 min with X+XO (0.1 mM xanthine plus 0.05 U/ml xanthine oxidase and 100 U/ml catalase) or for 3 hr with PQ^{2+} (150 μM), a redox-cycling agent capable of generating O_2^- intracellularly (Figures 1A and 1B).

To confirm that the decrease in aconitase activity by X+XO or PQ^{2+} was selective for aconitase and not due to a global effect on enzymes in the TCA cycle, we measured the activity of another TCA cycle enzyme, fumarase. Mammalian fumarase is functionally similar to aconitase but lacks an Fe–S center and is insensitive to inactivation by O_2^-. Cell lysates or cortical cells treated with X+XO and PQ^{2+}, respectively, showed decreased aconitase activity but no change in fumarase activity (Figure 1A).

The Fe–S center of aconitase is reversibly inactivated by O_2^-; i.e., it can be reactivated by addition of iron and reducing agents (Gardner and Fridovich, 1992; Flint et al., 1993; Gardner et al., 1995). To verify that aconitase inactivation by X+XO or PQ^{2+} in cortical cells results from generation of O_2^- and not from degradation of the protein, we asked whether aconitase inactivation by these agents was reversible. Cortical cells or cell lysates were treated with PQ^{2+} for 3 hr or with X+XO for 30 min, respectively; cells treated with PQ^{2+} were lysed, and aliquots of cell lysates incubated with vehicle or with a combination of dithiothreitol (DTT), sodium sulfide (Na_2S), and ferrous ammonium sulfate (FAS) (reactivation reagents) for 30 min. Recovery of purified aconitase under these conditions was used to verify the suitability of the reactivation assay. Aconitase activity was measured in vehicle-treated or reactivation reagent–treated cell lysates. Aconitase rendered inactive by X+XO or PQ^{2+} was completely reactivated by a 30 min incubation with reactivation reagents (Figure 1B). To test further the role of oxygen-derived radicals in aconitase inactivation, activity was measured in lysates whose aconitase was inactivated by oxygen in ambient air. Aconitase activity was measured in freshly prepared cell lysates, immediately and 24 hr after preparation (lysates were stored at 4°C for the 24 hr period). Aliquots of 24-hr-old lysates were analyzed for aconitase activity after incubation with reactivation buffer for 30 min. Aconitase activity was substantially decreased by 24 hr of exposure to ambient air and was reactivatable (Figure 1C).

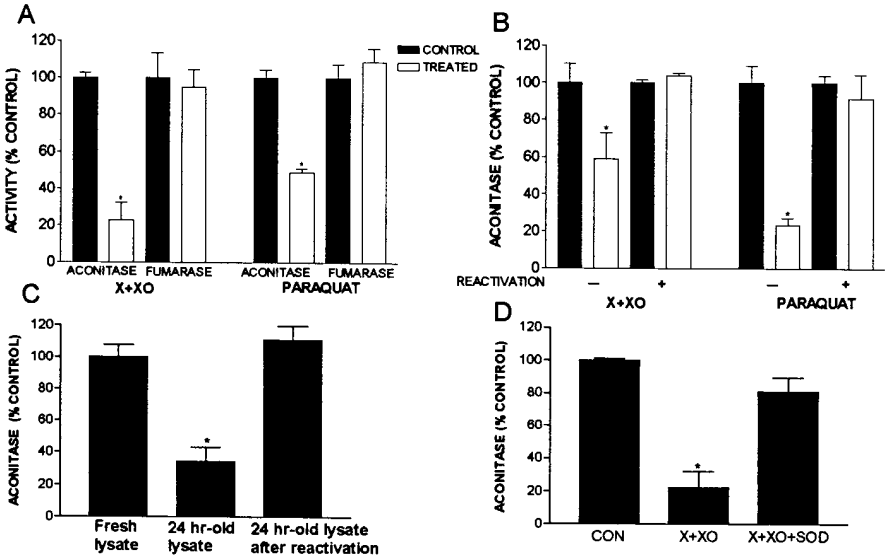

Figure 1. Validation of Aconitase Activity as a Marker for Superoxide

(A) Cortical cell lysates were treated with vehicle (control) or 0.1 mM xanthine plus 0.05 U/ml xanthine oxidase and 100 U/ml catalase (X+XO) for 30 min, and aconitase and fumarase activities were measured. Alternately, cortical cells were treated with vehicle (control) or 150 μM PQ^{2+} for 3 hr, and aconitase and fumarase activities were measured. Asterisks indicate a difference from all other treatments ($p < .05$, one-way ANOVA). Bars represent mean ± SEM ($n = 4$).

(B) Cortical cell lysates were treated with vehicle (control) or 0.1 mM xanthine plus 0.05 U/ml xanthine oxidase and 100 U/ml catalase (X+XO) for 30 min, after which lysates were incubated for 30 min with (+) or without (−) reactivation reagents (FAS, Na_2S, and DTT) and aconitase activity was measured. Alternately, cortical cells were treated with vehicle (control) or 150 μM PQ^{2+} for 3 hr, after which lysates were prepared and incubated for 30 min with (+) or without (−) reactivation reagents (FAS, Na_2S, and DTT) and aconitase activity was measured. Asterisks indicate a difference from all other treatments ($p < .05$, one-way ANOVA). Bars represent mean ± SEM ($n = 4$–6).

(C) Aconitase activity was measured in cortical cell lysates immediately after preparation (fresh lysate), in aliquots of the same lysates stored at 4°C for 24 hr (24-hr-old lysate), or in 24-hr-old lysates following a 30 min incubation with reactivation reagents. Asterisk indicates a difference from all other treatments ($p < .05$, one-way ANOVA). Bars represent mean ± SEM ($n = 3$).

(D) Aconitase activity was measured in cortical cell lysates treated with vehicle or 0.1 mM xanthine plus 0.05 U/ml xanthine oxidase and 100 U/ml catalase (X+XO) in the presence or absence of 100 U/ml SOD. Asterisk indicates a difference from all other treatments ($p < .05$, one-way ANOVA). Bars represent mean ± SEM ($n = 4$).

To verify that the inactivation of aconitase was due to O_2^- radicals, the ability of CuZnSOD to block X+XO-induced aconitase inactivation was tested. The generation of O_2^- by X+XO in cell-free lysates allowed the use of CuZnSOD here. Preincubation of cell lysates with CuZnSOD (100 U/ml) prevented the inactivation of aconitase induced by X+XO (Figure 1D), verifying a role for O_2^- in the mechanism of aconitase inactivation.

NMDA and KA Produce Reversible Inactivation of Aconitase with Distinct Time Courses

To determine whether glutamate receptor agonists produced a reversible inactivation of aconitase, the following experiments were performed. We determined the time course, Ca^{2+} dependence, selectivity, and reversibility of aconitase inactivation by NMDA. Parallel experiments were conducted for KA. The first detectable decrease of aconitase activity (22%) was evident after 15 min of exposure to 50 μM NMDA (Figure 2A). No change in aconitase was observed 5 min following NMDA treatment, and near maximal decrease (40%) was evident after 60 min. In contrast, the rate of inactivation of aconitase activity produced by 300 μM KA was markedly slower (Figure 2B). A small (10%) decrease was detected after 60 min of exposure, and near maximal decreases were evident after 4 hr (Figure 2B). Maximal decreases without overt cell loss were seen after 6 hr of exposure (Figure 2B).

Time points of 1 hr for NMDA and 6 hr for KA were chosen to investigate further parameters since robust decreases in aconitase activity were evident in the context of minimal cell loss as measured by ethidium homodimer-1 (EthD-1) staining (data not shown) at these times. Aconitase inactivation by both NMDA and KA was selective, since no reduction of fumarase activity occurred (Figure 2C), and was reversible by the addition of reactivation reagents (Figure 2D). Since the toxic effect of NMDA is dependent on the presence of extracellular Ca^{2+}, we determined whether aconitase inactivation by NMDA was Ca^{2+} dependent. Incubation of cells with 50 μM NMDA produced a larger decrease (30% change; $p < .05$, Student's t test) in aconitase activity in the presence of extracellular Ca^{2+} than in its nominal absence (10% change; no significant difference from control) (data not shown).

Aconitase Inactivation Produced by PQ^{2+}, NMDA, and KA Correlates with Cell Death

The time required by PQ^{2+}, NMDA, and KA for inactivation of aconitase (3, 1, and 6 hr, respectively) significantly precedes the death of neurons measured by lactate

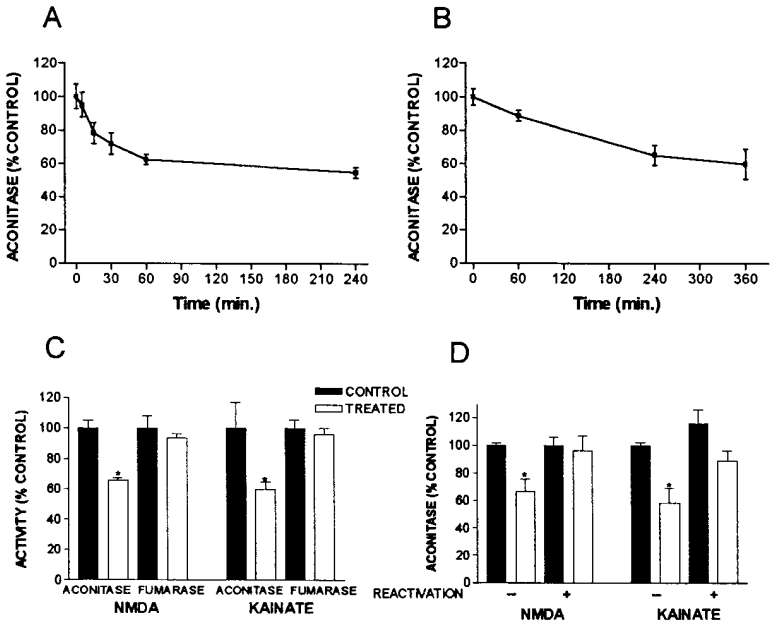

Figure 2. Characterization of NMDA- and KA-Induced Aconitase Inactivation

(A) Time course of NMDA-induced inactivation of aconitase. Cortical cells were treated with vehicle or 50 μM NMDA for 0, 5, 15, 30, 60, and 240 min, and aconitase activity was measured in cell lysates. Each point represents the mean ± SEM (n = 6–8).

(B) Time course of KA-induced aconitase inactivation. Cortical cells were treated with vehicle or 300 μM KA for 0, 60, 240, and 360 min, and aconitase activity was measured in cell lysates. Each point represents the mean ± SEM (n = 4–8).

(C) Selectivity of NMDA- and KA-induced aconitase inactivation. Cortical cells were treated with vehicle or 50 μM NMDA for 1 hr or with 300 μM KA for 6 hr. Aconitase and fumarase activities were measured in cell lysates. Asterisks indicate a difference from all other treatments ($p < .05$, one-way ANOVA). Bars represent the mean ± SEM (n = 3–6).

(D) Reversibility of NMDA- and KA-induced aconitase inactivation. Cortical cells were treated with vehicle or 50 μM NMDA for 1 hr or with 300 μM KA for 6 hr. Lysates were then prepared and incubated for 30 min with vehicle or reactivation reagents (FAS, Na_2S, and DTT), and aconitase activity was measured. Asterisks indicate a difference from all other treatments ($p < .05$, one-way ANOVA). Bars represent the mean ± SEM (n = 3–5).

dehydrogenase (LDH) release (18 hr) or evident by phase-contrast inspection. If O_2^- generation were necessary for neuronal death by these agents, then the aconitase inactivation would be expected to be proportionate to the degree of neuronal death. We therefore sought to determine whether aconitase inactivation and cell death produced by PQ^{2+}, NMDA, and KA correlated. Cortical cells were treated with varying concentrations of KA, NMDA, and PQ^{2+} for 18 hr, and the media were analyzed for LDH activity. Sister cultures were treated with varying concentrations of KA, NMDA, or PQ^{2+} for 6, 1, or 3 hr, respectively, and cell lysates were analyzed for aconitase activity; a shorter time of incubation was assessed for aconitase activity because death of neurons leads to irreversible inactivation of aconitase activity, presumably owing to protein degradation. Therefore, an earlier time point was selected for measuring aconitase activity based upon the time of approximating the steady state of reversible inactivation (Figures 2A and 2B for 50 μM NMDA and 300 μM KA, respectively; data not shown for PQ^{2+}).

KA treatment produced proportionate decreases in aconitase activity and cell death as monitored by LDH release (Figure 3A). Likewise, PQ^{2+} treatment produced a proportionate decrease of aconitase activity and the amount of LDH release (Figure 3B). At higher concentrations (30–1000 μM), NMDA produced a proportionate decrease in aconitase activity and cell death. However, low concentrations (3 and 10 μM) of NMDA produced cell death (LDH release) but no detectable aconitase inactivation (Figure 3C). Since aconitase activity and LDH release were measured 1 and 18 hr, respectively, after initiation of NMDA exposure, the possibility emerged that lower concentrations of NMDA may require longer exposure times to produce the decrease in aconitase activity. To test this possibility, we measured aconitase activity in lysates prepared from cells incubated with 10 μM or 1 mM NMDA for 1, 2, 3, 4, and 6 hr. Measurement of aconitase activity at 6 hr revealed a 43% and 47% reduction induced by 10 μM and 1 mM NMDA, respectively (control: 23.4 ± 1.4 U/g of aconitase activity; 10 μM NMDA: 13.4 ± 2.4 U/g; 1 mM NMDA: 12.4 ± 0.7 U/g; n = 4). Therefore, it seems likely that the increased LDH release in the absence of aconitase inactivation detected at 3 and 10 μM NMDA (Figure 3C) can be explained by the time points selected for the study. Taken together, a good correlation was found between the degree of aconitase inactivation and the amount of cell death as measured by LDH release by each of these treatments.

Correlating aconitase activity with LDH release highlighted an additional discrepancy between the concentration–response curves for PQ^{2+}, KA, and NMDA. That is, a discrepancy in the absolute amounts of LDH and aconitase inactivation induced by the various treatments was found. PQ^{2+} almost totally inactivated aconitase activity yet produced only a 2-fold increase of LDH. By contrast, NMDA produced only a 40% reduction of aconitase activity yet a 4-fold increase of LDH activity. KA also produced a 40% reduction of aconitase activity and a 3-fold increase of LDH activity. Potential explanations for this discrepancy are addressed in the Discussion.

The SOD Mimetic MnTBAP Prevents Aconitase Inactivation and Cell Death Produced by PQ^{2+}, NMDA, and KA

Together, these results are consistent with the hypothesis that O_2^- radicals are in the pathway mediating the toxicities of PQ^{2+}, NMDA, and KA. To test this hypothesis

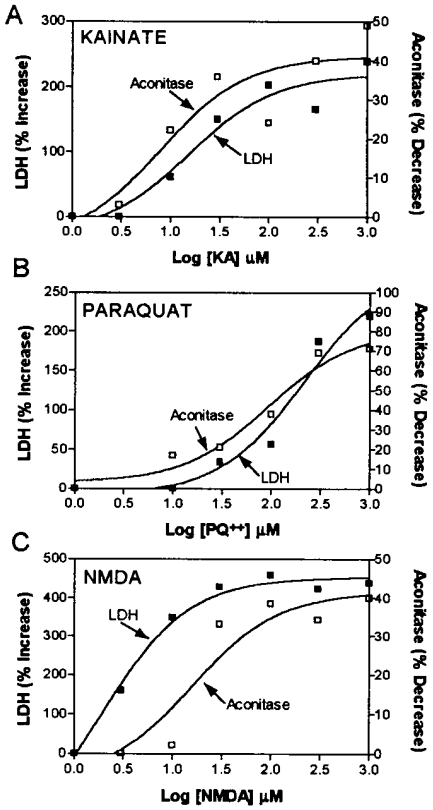

Figure 3. Correlation of Toxicity with Aconitase Inactivation

Concentration dependence of KA (A), PQ^{2+} (B), and NMDA (C) to induce toxicity (left axis) and aconitase inactivation (right axis) were determined. Values were normalized as a percentage of LDH release (closed squares) or aconitase inhibition (open squares) and plotted to assess the correlation between LDH release and aconitase inactivation. Curves were computer generated using nonlinear regression analysis using the equation (GraphPad Prism):

$$Y = \text{Bottom} + (\text{Top} - \text{Bottom})/(1+10^{\text{LogEC50} - X}).$$

Each point represents the mean value (n = 4–6).

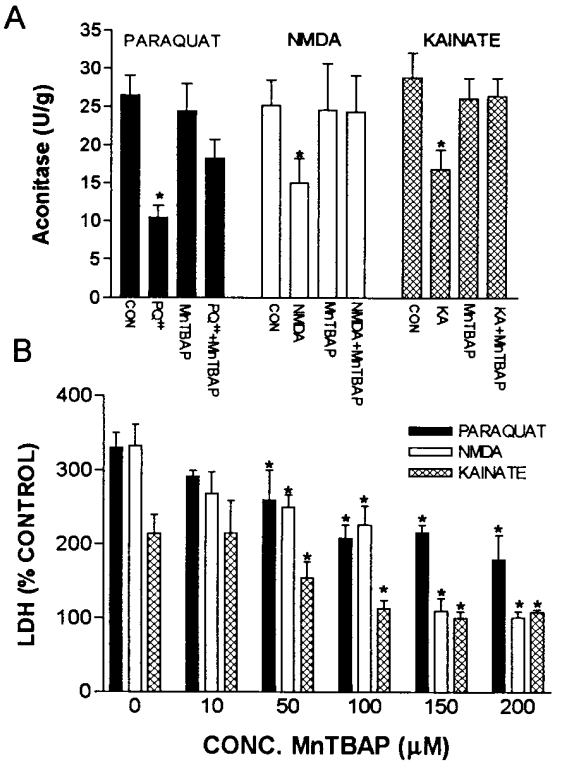

Figure 4. Effect of MnTBAP on NMDA-, KA-, and PQ^{2+}-Induced Aconitase Inactivation and Cell Death

(A) Blockade of aconitase inactivation by MnTBAP. Cortical cells were treated with 150 μM PQ^{2+} for 3 hr (solid bars), 50 μM NMDA for 1 hr (open bars), or 300 μM KA for 6 hr (hatched bars) in the presence or absence of 200 μM MnTBAP (present 15 min prior to and throughout the duration of treatment), and aconitase activity was measured in cell lysates. Bars represent mean ± SEM (n = 8–12). Asterisks indicate a difference from all other treatments ($p < .05$, one-way ANOVA).

(B) Blockade of neurotoxicity by MnTBAP. Cortical cells were treated with 150 μM PQ^{2+} (solid bars), 50 μM NMDA (open bars), or 300 μM KA (hatched bars) in the presence of varying concentrations of MnTBAP (present 15 min prior to and throughout the duration of treatment) for 18 hr, and LDH release was measured in the medium. Asterisks represent a difference from controls (agonist in the absence of MnTBAP; $p < .05$ Dunnet's test). Bars represent mean ± SEM (n = 3–6).

further, the effects of the cell-permeable SOD mimetic MnTBAP were examined. The goals of these experiments were to determine whether MnTBAP can prevent aconitase inactivation and cell death produced by PQ^{2+}, NMDA, and KA; whether a structurally distinct porphyrin with 10-fold lower SOD activity lacks the ability to protect cells from O_2^--mediated responses; and whether addition of MnTBAP after excitotoxic insult can rescue neurons.

To determine whether MnTBAP can prevent aconitase inactivation and cell death produced by NMDA, PQ^{2+}, and KA, cortical cells were incubated with PQ^{2+}, NMDA, and KA in the absence and presence of 200 μM MnTBAP. PQ^{2+}, NMDA, and KA produced a 70%, 40%, and 42% decrease in aconitase activity after 3, 1, and 6 hr, respectively; 200 μM MnTBAP markedly inhibited the PQ^{2+}-, NMDA-, and KA-mediated decreases of aconitase activity (Figure 4A). Parallel effects were evident on cell death as measured by LDH release. MnTBAP (200 μM) markedly inhibited PQ^{2+}-, NMDA-, and KA-mediated cell death (Figure 4B). The effects of MnTBAP on cell death were concentration dependent (Figure 4B). MnTBAP (200 μM) produced a rightward and downward shift in the concentration–response curve for NMDA, providing complete protection at low concentrations of NMDA (Figure 5).

To exclude the possibility that MnTBAP simply prevented activation of NMDA or AMPA receptors, the effect of MnTBAP on NMDA- and KA-induced Ca^{2+} influx was examined using the Ca^{2+}-sensitive indicator dye Fura 2. Three consecutive stimulations of 50 μM NMDA, spaced 15 min apart, produced changes in peak $[Ca^{2+}]_i$ of 214 ± 44 nM, 179 ± 37 nM, and 166 ± 43 nM (n = 12). In the presence of 200 μM MnTBAP (present 15 min prior to as well as during the second NMDA stimulation), three consecutive stimulations of 50 μM NMDA also produced changes in peak $[Ca^{2+}]_i$ of 222 ± 19 nM, 169 ± 19 nM, and 162 ± 11 nM (n > 12; no statistical differences between the presence and absence of MnTBAP were found by one-way ANOVA). Since repeated stimulations

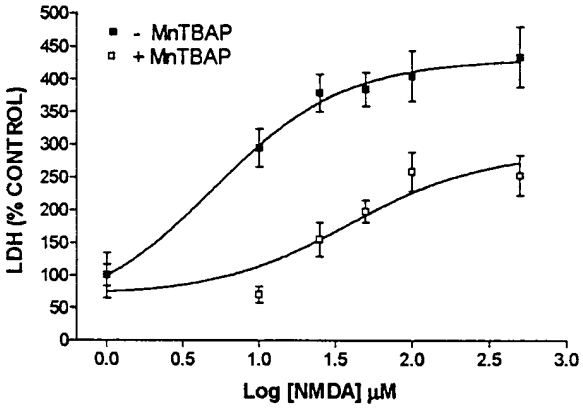

Figure 5. Inhibition of NMDA Toxicity by MnTBAP

Cortical cells were treated with varying concentrations of NMDA in the presence and absence of 200 μM MnTBAP for 18 hr, and LDH was measured in media. Each point represents mean ± SEM (n = 3–4.)

of KA produced attenuation of Ca^{2+} increases, the effect of MnTBAP on KA-induced Ca^{2+} influx was examined in separate sister cultures. KA (300 μM) produced changes in peak $[Ca^{2+}]_i$ of 213 ± 45 nM and 185 ± 27 nM (n = 8–12) in the absence and presence of 200 μM MnTBAP, respectively (no statistical difference detected by Student's t test). Hence, MnTBAP had no significant effect on either NMDA- or KA-induced Ca^{2+} influx.

To strengthen the possibility that MnTBAP decreased aconitase inactivation and prevented cell death by its SOD-mimetic action, we examined the effects of a structurally related congener with diminished SOD activity. The SOD activity of MnTBAP is dependent on cyclic catalysis by the manganese moiety. Substitution of manganese with zinc in the porphyrin structure of MnTBAP (ZnTBAP) results in 10-fold less SOD activity (Day et al., 1995). EthD-1 was used to quantitate cell death in these experiments because preliminary studies showed that ZnTBAP interfered with the measurement of LDH (MnTBAP was found to have no effect on LDH measurement). Concentration–response curves for NMDA and KA demonstrated a strong correlation between cell death measured using LDH release and dead cells quantitated by EthD-1. Concentration–response curves disclosed that MnTBAP exhibited markedly increased neuroprotective effects in comparison with ZnTBAP against PQ^{2+}, NMDA, and KA toxicities (Figure 6).

To determine whether addition of MnTBAP after initiation of the excitotoxic insult exerted neuroprotective effects, the following experiments were performed. In contrast to experiments previously described in this paper, in which 50 μM NMDA was included for 18 hr in MEM-g (chronic exposure paradigm), the experiments described here include 100 μM NMDA for 15 min (acute exposure paradigm) in $HBSS^+$ (Ca^{2+}- and Mg^{2+}-free HBSS containing 5.6 mM glucose and supplemented with 2 mM $CaCl_2$, 1 mM $NaHCO_3$, 10 mM HEPES, and 5 μM glycine). This acute exposure paradigm induced delayed neuronal death (measured 18 hr later) and allowed us to determine the temporal relationship between MnTBAP exposure and neuroprotection. The neuroprotective effects of MnTBAP were assessed when it

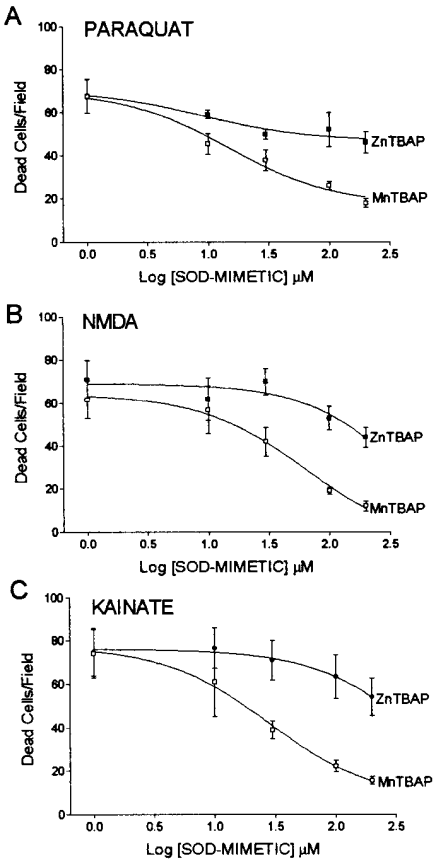

Figure 6. Differential Effect of MnTBAP and ZnTBAP on Cell Death

Cortical cells were treated with 150 μM PQ^{2+} (A), 50 μM NMDA (B), or 300 μM KA (C) in the presence or absence of varying concentrations of MnTBAP (open squares) or ZnTBAP (closed squares), and dead cells were stained with EthD-1. Images of EthD-1-positive cells were stored and counted in randomly selected fields using a digital image analyzer. Data are expressed as the number of dead cells per field. Each point represents measurements made from 1200–1500 cells.

was: present 15 min prior to and during a 15 min NMDA application (but not for the 18 hr period after medium change; Figure 7A, condition "Pre"); present 15 min prior to and during a 15 min NMDA application and for the ensuing 18 hr (Figure 7A, condition "Pre+Post"); added 15, 30, or 60 min following a 15 min incubation with 100 μM NMDA and left in the media for the ensuing 18 hr (Figure 7B). Condition Pre (Figure 7A) resulted in a 25% reduction of LDH release measured 18 hr later; using an identical time course of application of 100 μM D-amino-5-phosphonovalerate (D-APV) in condition Pre, a complete blockade of LDH release was observed (Figure 7A). In contrast, MnTBAP incubated as in condition Pre+Post resulted in a 51% reduction of LDH release (Figure 7A). Addition of 200 μM MnTBAP 15, 30, or 60 min following a 15 min exposure to 100 μM NMDA (Figure 7B) resulted in a 38%, 30%, and 25% reduction of LDH release, respectively. In contrast, addition of 10 μM MK801 had a modest protective effect (17%) when added 15 min after the NMDA insult.

Since peroxynitrite, a reaction product of O_2^- and nitric

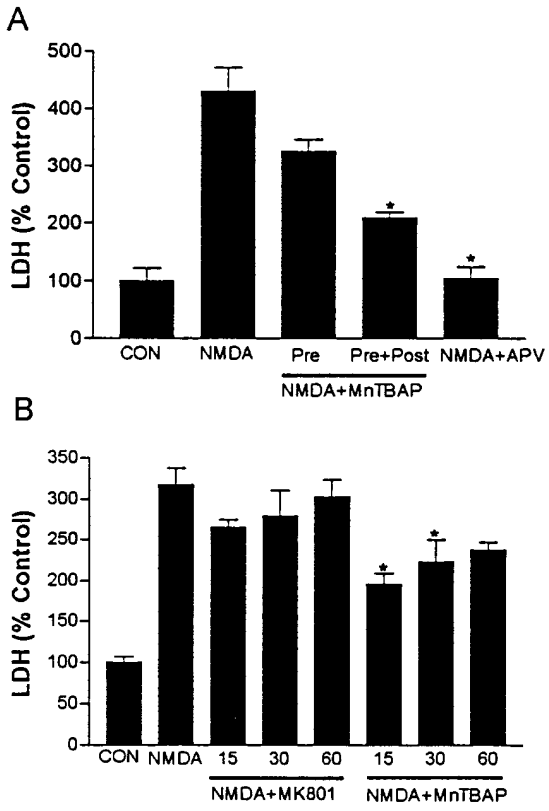

Figure 7. Effect of MnTBAP on NMDA-Induced Cell Death

(A) Inhibition of NMDA toxicity by MnTBAP. Cortical cells were incubated for 15 min with vehicle (CON) or 100 μM NMDA alone or in the presence of 200 μM MnTBAP or 100 μM D-APV (present 15 min prior to and during NMDA exposure) in $HBSS^+$, followed by medium change to MEM-g for 18 hr; LDH was measured in the supernatant medium (Pre). Alternately, cortical cells were preincubated with 200 μM MnTBAP for 15 min, incubated with 100 μM NMDA plus 200 μM MnTBAP for 15 min in $HBSS^+$, followed by medium change to MEM-g containing 200 μM MnTBAP for 18 hr (Pre+Post). Asterisks indicate a difference from NMDA treatment ($p < .05$, one-way ANOVA). Bars represent mean ± SEM ($n = 4–6$).

(B) Rescue of NMDA toxicity by MnTBAP. Cortical cells were treated with vehicle (CON) or 100 μM NMDA for 15 min in $HBSS^+$ and returned to MEM-g. Vehicle, 200 μM MnTBAP, or 10 μM MK801 was added to cells 15, 30, and 60 min after medium change, and LDH was measured 18 hr thereafter. Asterisks indicate a difference from NMDA treatment ($p < .05$, one-way ANOVA). Bars represent mean ± SEM ($n = 4–6$).

oxide, can inactivate aconitase (Hausladen and Fridovich, 1994) and contribute to NMDA-induced neuronal death (Dawson et al., 1991; Lipton et al., 1993), the possibility emerged that NMDA-induced aconitase inactivation may result at least in part from peroxynitrite formation. To investigate this possibility, we assessed the effects of nitric oxide synthase (NOS) inhibitors on NMDA-induced aconitase inactivation and cell death. NMDA-induced aconitase inactivation and LDH release were unchanged by the presence of of either N^G-nitro-L-arginine methyl ester, N^G-nitro-L-arginine, or N^G-monomethyl-L-arginine (each at 1 mM; data not shown). To determine whether NOS was expressed in our cortical neuronal preparation, immunocytochemical analyses were performed using a polyclonal antibody to neuronal NOS. Approximately 2% of the cortical cells exhibited immunoreactivity for neuronal NOS (data not shown), a result consistent with the findings of Dawson et al. (1993). Together, these data argue against an etiological role for peroxynitrite in NMDA-induced aconitase inactivation or cell death under the conditions used here.

Discussion

Four principal findings emerge from this work. First, two distinct O_2^- generators selectively inactivate aconitase by a posttranslational mechanism, as demonstrated by reversibility of the inactivation with iron and a reducing agent. Second, exposure to excitotoxic concentrations of either NMDA or KA produces selective decreases of aconitase activity, which precede and correlate quantitatively with induction of cell death. Third, the cell-permeable SOD mimetic, MnTBAP, prevents both decreases of aconitase activity and cell death produced by PQ^{2+}, NMDA, and KA. Finally, ZnTBAP, a congener of MnTBAP with 10-fold less SOD activity, exhibits markedly diminished protective effects against PQ^{2+}-, NMDA-, and KA-induced decreases of aconitase activity and cell death. We draw the following conclusions from these four findings. Decreases of aconitase activity that are reversible by iron and reducing agents provide a measure of intracellular O_2^- generation. Excitotoxic consequences of both NMDA and KA are preceded by and correlate with intracellular O_2^- generation. MnTBAP exerts its neuroprotective effects by scavenging O_2^- radicals. Together, these findings provide direct evidence that the formation of O_2^- radicals is an obligate step in the intracellular events culminating in excitotoxic death of cortical neurons. Although O_2^- radical formation is an obligate step in excitotoxic injury, whether O_2^- itself or some derivative of O_2^- (such as peroxynitrite or hydroxyl radical) is the ultimate toxicant remains to be resolved.

Aconitase Activity as a Measure of Intracellular O_2^- Generation

Aconitase activity has recently been shown to be a sensitive and specific indicator of intracellular O_2^- generation in E. coli (Gardner and Fridovich, 1991, 1992; Hausladen and Fridovich, 1994) as well as mammalian cells (Gardner et al., 1995). Since aconitase is a physiological intracellular target of O_2^- and its reaction product peroxynitrite, its usefulness as an O_2^- detector has some advantages over currently available methods, which rely on the use of exogenously added indicator agents such as spin traps and redox-sensitive dyes that could perturb cell structure and function. Redox-sensitive dyes offer the advantage of detecting oxygen radicals in real time within live cells but lack the selectivity for O_2^- radicals. EPR spectroscopy with spin traps is a sensitive method of O_2^- measurement but has some disadvantages associated with its use. Most spin traps currently available form O_2^- adducts that are relatively unstable. Moreover, the spin traps have a low rate of reaction with O_2^- ($k_T \approx 10\ M^{-1}s^{-1}$), requiring the use of very high concentrations of spin traps compared with SOD (Halliwell and Gutteridge, 1989a), which may perturb cell structure and function.

The following observations support the view that aconitase activity can be used as a valid marker for O_2^- measurement in cortical cultures. One is the inactivation of aconitase by known O_2^- generators such as X+XO and PQ^{2+}. This is consistent with the idea that O_2^- is sufficient to inactivate aconitase. A second is the blockade of X+XO-induced inactivation of aconitase by SOD. This provides insight into the mechanism of the inactivation. The specificity inherent in this enzyme implies that X+XO inactivation is mediated by O_2^- radicals. A third is the selective inactivation of aconitase but not the alternate TCA cycle enzyme, fumarase. Since fumarase activity remains unchanged in lysates whose aconitase is inactivated by treatment with X+XO or PQ^{2+}, the effect of these treatments is specific for aconitase and not due to a global effect on TCA cycle enzymes. A fourth is the reversibility of aconitase inactivation achieved by FAS, Na_2S, and DTT. This demonstrates that the mechanism of inactivation is posttranslational and, together with data from E. coli (Gardner and Fridovich, 1991, 1992), implies that reversibility involves restoration of the Fe–S center of aconitase. Importantly, since both X+XO and PQ^{2+} generate some hydrogen peroxide and hydroxyl radicals as derivatives of O_2^-, it is possible that their effects are mediated by a combination of ROS.

Excitotoxic Concentrations of NMDA and KA Evoke O_2^- Radical Formation

Using reversible inactivation of aconitase as a marker of O_2^- radical formation, we were able to demonstrate that both NMDA and KA generated O_2^- radicals. NMDA-induced aconitase inactivation followed a rapid time course (occurring within 15 min of exposure) and was Ca^{2+} dependent, a profile identical to the toxicity of NMDA in neuronal cultures. This is in agreement with NMDA receptor–mediated increases in ROS detected in cerebellar granule cells (Lafon-Cazal et al., 1993) and forebrain neurons (Reynolds and Hastings, 1995). The ability of KA to generate O_2^- is in contrast with the findings of Lafon-Cazal et al. (1993); the difference probably reflects the length of time of KA exposure. Our experiments suggest that KA requires several hours of exposure to decrease aconitase activity and induce cell death; a 30 min incubation time as used by Lafon-Cazal et al. (1993) was not sufficient. The time course of KA-mediated reductions of aconitase activity correlated closely with the toxicity profile of non-NMDA agonists in neuronal cultures (Koh et al., 1990). The demonstration that KA increases O_2^- production provides direct evidence supporting the emerging role of free radicals in non-NMDA receptor–mediated toxicity in vitro (Dykens et al., 1987; Puttfarcken et al., 1993; Cheng and Sun, 1994).

The inability of NOS inhibitors to protect against NMDA-induced aconitase inactivation and cell death argues against a major role for peroxynitrite in mediating the effects of NMDA under the conditions used here. Peroxynitrite may play an important role in NMDA-induced aconitase inactivation under conditions in which the inducible form of NOS is activated by cytokines, as has been found by Hewett et al. (1994).

The source of O_2^- generation following an excitotoxic insult is presently unknown. Mitochondria have recently been demonstrated to be a major source of ROS following NMDA receptor activation (Reynolds and Hastings, 1995). Of the several distinct Ca^{2+}-requiring enzymes, phospholipase A_2 is an attractive candidate as a source of O_2^- formation following NMDA receptor activation (Dumius et al., 1988; Lafon-Cazal et al., 1993). Activation of phospholipase A_2 hydrolyzes membrane lipids to free fatty acids including arachidonic acid: O_2^- radicals can be generated as by-products of arachidonic acid metabolism (Halliwell and Gutteridge, 1989b).

O_2^- Radical Formation Is Necessary for Both NMDA- and KA-Induced Death of Cortical Neurons

Plotting the concentration–response curves for NMDA-, KA-, and PQ^{2+}-induced aconitase inactivation and LDH release allowed us to examine both the qualitative and quantitative relationship between O_2^- generation and cell death. Although this study does not directly test or demonstrate a causal role of aconitase inactivation in cell death, it revealed an important correlation between these parameters. In the case of KA and PQ^{2+}, the curves for aconitase inactivation and cell death closely paralleled each other, suggesting a causal role for aconitase inactivation (O_2^- generation) in cell death. In contrast, low concentrations NMDA were more effective at inducing cell death than aconitase inactivation. However, the demonstration that a low concentration of NMDA (10 μM) requires several hours of exposure for aconitase inactivation argues in favor of a causal role for O_2^- in inducing cell death.

The quantitative discrepancies between aconitase inactivation and the magnitude of LDH release produced by NMDA, KA, and PQ^{2+} are noteworthy. Although our data support the idea that O_2^- radical formation is required for the cell death produced by these treatments, these quantitative discrepancies between aconitase inactivation and LDH release imply that O_2^- radical formation is not sufficient to explain all of the toxic consequences of these various treatments. One explanation may be that other signal transduction cascades activated by NMDA and KA are of pivotal importance in determining the magnitude of cell death. The ability of MnTBAP to prevent aconitase inactivation and cell death induced by NMDA and KA supports a role for O_2^- generation in their toxic effects.

In addition to serving as a marker of O_2^- production, the positive correlation observed here between aconitase inactivation and cell death led us to speculate that aconitase inactivation itself may be a pivotal step in cell death produced by PQ^{2+} and excitotoxic agents. There are two mechanisms by which aconitase inactivation might lead to cell death. First, inactivation of this key enzyme in the TCA cycle can disrupt mitochondrial energy production, leading to energy depletion and cell death. Second, the reaction whereby aconitase undergoes inactivation by O_2^- yields Fe(II) and hydrogen peroxide (see equation 1 in Introduction), which can further undergo Fenton chemistry, leading to the generation of the toxic hydroxyl radical species, and thus contribute to excitotoxic injury (Lafon-Cazal et al., 1993).

The time course of NMDA-induced aconitase inactivation is consistent with the idea that O_2^- radicals are

generated throughout the excitotoxic process. Maximal beneficial effects of MnTBAP were observed when it was present before, during, and after NMDA exposure rather than only before and during an acute (15 min) exposure. The fact that delayed addition of MnTBAP was able to protect against an acute NMDA insult further suggests that its action is to interfere with the deleterious cascade triggered by the excitotoxic exposure that ultimately produces cell death.

Specificity of MnTBAP Action

The present studies support the idea that the protective effects of MnTBAP are related to its SOD-mimetic actions and are in agreement with previous studies demonstrating its protective effects against PQ^{2+}-induced damage to E. coli (Faulkner et al., 1994) as well as to mammalian cells (Day et al., 1995). The inability of the less active congener, ZnTBAP, to protect cortical cells against PQ^{2+}-, NMDA-, and KA-induced toxicity is in agreement with its inability to protect lung cells from PQ^{2+} toxicity (Day et al., 1995) and strengthens the likelihood that SOD-mimetic action underlies the protective effects afforded by MnTBAP. The SOD activity of MnTBAP is dependent on cyclic redox changes in the manganese moiety. Replacement of manganese in the porphyrin structure with zinc, a metal that does not readily change its valence, resulted in a 10-fold decreased SOD activity and in the protective actions seen here and reported previously (Day et al., 1995). The site at which MnTBAP exerts its SOD-mimetic actions is likely intracellular, based on two observations. First, MnTBAP protects cells against aconitase inactivation and cell death induced by PQ^{2+}, an intracellular redox-cycling agent (Bus and Gibson, 1984). Second, MnTBAP can be transported into cultured endothelial cells (Day et al., 1995). The lack of effect of MnTBAP on NMDA- and KA-induced Ca^{2+} influx suggests that its action is beyond the membrane-bound NMDA and AMPA/KA receptors and implies that the site of its action centers on postreceptor events leading to excitotoxicity.

In summary, the significance of this work is 2-fold. First, we have demonstrated a posttranslational modification of aconitase, an important TCA cycle enzyme, following glutamate receptor activation. Although further studies are required, it is tempting to speculate that aconitase and possibly other Fe–S-containing enzymes may be important targets involved in mediating pathological consequences of glutamate receptor activation. Second, we not only show that NMDA and KA produce O_2^- but that O_2^- production correlates with excitotoxic damage and is required for it. These observations provide an important mechanistic link between O_2^- radical formation and glutamate excitotoxicity as well as offer a pharmacological strategy (SOD mimetic such as MnTBAP) for blocking distal pathways mediating neurodegeneration in various disease states. Since superoxide radicals also serve physiological roles (Halliwell and Gutteridge, 1989b), pharmacological strategies aimed at controlling superoxide radical concentrations must be carefully designed and implemented to minimize unwanted effects.

Experimental Procedures

Tissue Culture

Mixed neuronal and glial cultures were prepared from embryonic day 18 rat cerebral cortices (Sprague–Dawley, Zivic Miller). In brief, the cerebral cortices were dissected and enzymatically dissociated by incubation in Ca^{2+}- and Mg^{2+}-free HBSS supplemented with 10 mM HEPES and 0.25% trypsin for 20 min at 37°C. The tissue was rinsed and dispersed into single-cell suspension by gentle passage through a fire-polished Pasteur pipette. The cell suspension was centrifuged and resuspended in Minimum Essential Media (MEM) containing Earle's salts supplemented with 3 g/l glucose, 5% horse serum, and 5% fetal bovine serum (growth medium). The cells were plated in poly-D-lysine-coated multiwell plates: 12-well plates (for aconitase measurement), 24-well plates (for toxicity experiments), and 22 mm glass coverslips (for Ca^{2+} measurements). Cells were maintained at 37°C in a humidified incubator with 5% CO_2/95% air in growth medium. Medium was not replaced so as to reduce glial overgrowth and neuronal loss. Mature cells (14–17 days in vitro) were used for all experiments.

Cell Treatment

The growth medium was replaced with MEM supplemented with 25 mM glucose (MEM-g). For both neurotoxicity studies and aconitase measurement, cells were incubated in the designated treatment for the indicated length of time at 37°C. Unless otherwise specified, antagonists or SOD mimetics were added 15 min prior to agonists. For measurement of neurotoxicity, cells were incubated with treatments for 18 hr at 37°C in MEM-g. To assess the ability of antagonists to inhibit acute NMDA toxicity or rescue cells from an ongoing NMDA insult, an alternate paradigm of NMDA treatment was used in addition to the one described above. In this paradigm, growth medium was replaced with $HBSS^+$ (Ca^{2+}- and Mg^{2+}-free HBSS supplemented with 2 mM $CaCl_2$, 1 mM $NaHCO_3$, 10 mM HEPES, and 5 μM glycine); cells were treated with vehicle or 100 μM NMDA for 15 min, after which $HBSS^+$ was replaced with MEM-g; and cells were returned to the incubator for an additional 18 hr. Antagonists or SOD mimetics were added to the cells 15 min before NMDA exposure or 15, 30, or 60 min following final medium replacement. For determination of Ca^{2+} dependence, cells were incubated in $HBSS^+$ with no added Ca^{2+}. When KA was used as an agonist, 100 μM D-APV was routinely included to block secondary NMDA receptor activation. Catalase (100 U/ml) was always included when X+XO was used as a treatment to rule out the contribution of hydrogen peroxide.

Neurotoxicity Studies

Neurotoxicity was determined by the measurement of LDH released in the supernatant media as previously described (Patel et al., 1991, 1992). LDH was measured by the method of Vassault (1983). Additionally, cell death was confirmed with EthD-1 as an indicator of dead cells. In brief, the cells were washed twice with HBSS, loaded with 20 μM EthD-1 for 30 min, rinsed twice, and viewed through fluorescence optics. The number of dead cells labeled with EthD-1 were counted in 4–6 randomly selected fields, the numbers were averaged to give an estimate of cell death, and the experiment was repeated three times. Each field contained 80–100 cells, and for each observation a total of 1200–1500 cells were counted.

Aconitase and Fumarase Measurement

For the measurement of aconitase and fumarase activities, following treatment with agents, media were removed and cells were lysed in ice-cold 50 mM Tris–HCl (pH 7.4) containing 0.6 mM $MnCl_2$, 1 mM L-cysteine, 1 mM citrate, and 0.5% Triton-X 100. The aconitase activity of cell lysates was measured spectrophotometrically by monitoring the formation of cis-aconitate from isocitrate at 240 nm in 50 mM Tris–HCl (pH 7.4) containing 0.6 mM $MnCl_2$ and 20 mM isocitrate at 25°C (Krebs and Holzach, 1952; Gardner and Fridovich, 1992). Inactive aconitase was reactivated by a 30 min incubation of cortical cell lysates (90 μl) with 0.5 M DTT (10 μl), 20 mM Na_2S (1 μl), and 20 mM FAS (1 μl) in 50 mM Tris–HCl (pH 8.0) at 37°C. Aconitase activity in cortical cell lysates was inhibited by 0.1 mM potassium ferricyanide or by boiling the sample. Fumarase activity was measured by monitoring the increase in absorbance at 240 nm

at 25°C in a 1 ml reaction mixture containing 30 mM potassium phosphate, 0.1 mM EDTA, and 5 mM L-malate (pH 7.4) (Racker, 1950). Fumarase activity in cortical cell lysates showed stereospecificity for L-malate; D-malate was inactive. Protein concentrations were measured using Coomassie Plus reagents (Pierce).

Ca^{2+}_i Measurement

Ca^{2+}_i was measured using the Ca^{2+} indicator dye Fura 2, as described previously (Lerea et al., 1992). In brief, dye-loaded cells were stimulated three consecutive times by vehicle or NMDA, and the change in Fura 2 fluorescence ratio (340/380 nm) was monitored by a digital imaging system (Universal Imaging Inc.) interfaced with a Zeiss microscope. Stimulations of cells were spaced by 15 min intervals and three washes. The first stimulation established the responsiveness of cells so that inhibitors could be tested during the second stimulation and recovery of cells tested during the third stimulation. Comparisons were made of the three consecutive NMDA responses in the presence of vehicle or MnTBAP. Repeated stimulations with KA resulted in significantly diminished responses during repeated stimulations, presumably due to desensitization of voltage-sensitive Ca^{2+} channels; hence, for measuring Ca^{2+} responses using KA as the agonist, cells from sister cultures grown on separate coverslips were treated with a single stimulation of KA in the presence of vehicle or MnTBAP. Ca^{2+}_i concentrations were calculated from 340/380 nm ratio changes following in vitro calibrations using Ca^{2+} standards.

Immunocytochemistry

Cells were fixed with 4% paraformaldehyde and incubated at 4°C overnight with polyclonal rabbit anti-NOS (1:500 dilution of anti-NOS raised against rat cerebellum; Ferid Murad, IL). The cells were washed and incubated with secondary antibody (1:200 biotinylated anti-rabbit IgG; Vector Labs.) for 1 hr at 25°C and processed for immunocytochemistry.

Statistical Analyses

One-way ANOVA was used to compare three or more treatments and Dunnet's test for comparing multiple treatment groups with a control group. Tukey–Kramer multiple comparisons test was used to detect differences between treatments. Student's t test was used for comparison of two treatments.

Reagents

Excitatory amino acid agonists and antagonists were obtained from Tocris Cookson. Catalase and xanthine oxidase were obtained from Boerhinger Mannheim. EthD-1 and Fura 2–AM were obtained from Molecular Probes. MnTBAP and ZnTBAP were synthesized as described previously (Day et al., 1995). Tissue culture reagents were obtained from GIBCO. All other reagents were obtained from Sigma Chemical Co.

Acknowledgments

The authors would like to thank Dr. Alfred Hausladen for helpful discussions regarding aconitase measurement. This work was supported by grants from the National Institutes of Health (NS 32334 [J. O. M.]; PO1 HL31992 [J. D. C.]) and the Epilepsy Foundation of America (M. P.).

The costs of publication of this article were defrayed in part by the payment of page charges. This article must therefore be hereby marked *"advertisement"* in accordance with 18 USC Section 1734 solely to indicate this fact.

Received August 11, 1995; revised October 23, 1995.

References

Bus, J.S., and Gibson, J.E. (1984). Paraquat: model for oxidant-initiated toxicity. Environ. Health Perspect. *55*, 37–46.

Chan, P.H., Chu, B.S., Chen, S.F., Carlson, E.J., and Epstein, C.J. (1990). Reduced neurotoxicity in transgenic mice overexpressing human copper-zinc-superoxide dismutase. Stroke *21*, 80–82.

Cheng, Y., and Sun, A.Y. (1994). Oxidative mechanisms involved in kainate-induced cytotoxicity in cortical neurons. Neurochem. Res. *19*, 1557–1564.

Choi, D.W. (1985). Glutamate neurotoxicity in cortical cell culture is calcium dependent. Neurosci. Lett. *58*, 293–297.

Choi, D.W. (1988). Glutamate neurotoxicity and diseases of the nervous system. Neuron *1*, 623–634.

Coyle, J.T., and Puttfarcken, P. (1993). Oxidative stress, glutamate, and neurodegenerative disorders. Science *262*, 689–695.

Dawson, V.L., Dawson, T.M., London, E.D., Bredt, D.S., and Snyder, S.H. (1991). Nitric oxide mediates glutamate neurotoxicity in primary cortical cultures. Proc. Natl. Acad. Sci. USA *88*, 6368–6371.

Dawson, V.L., Dawson, T.M., Bartley, D.A., Uhl, G.R., and Snyder, S.H. (1993). Mechanisms of nitric oxide-mediated neurotoxicity in primary brain cultures. J. Neurosci. *13*, 2651–2661.

Day, B.J,. Shawn, S., Liochev, S.I., and Crapo, J.D. (1995). A metalloporphyrin superoxide dismutase mimetic protects against paraquat-induced endothelial cell injury, *in vitro*. J. Pharmacol. Exp. Ther. *275*, 1227–1232.

Dumius, A., Sebban, M., Haynes, L., Pin, J.P., and Bockaert J. (1988). NMDA receptors activate the arachidonic acid cascade system in striatal neurons. Nature *336*, 68–70.

Dykens, J.A., Stern, A., and Trenkner, E. (1987). Mechanism of kainate toxicity to cerebellar neurons *in vitro* is analogous to reperfusion injury. J. Neurochem. *49*, 1222–1228.

Faulkner, K.M., Liochev, S.I., and Fridovich, I. (1994). Stable Mn(III) porphyrins mimic superoxide dismutase activity *in vitro* and substitute for it *in vivo*. J. Biol. Chem. *269*, 23471–23476.

Flint, D.H., Tuminello, J.F., and Emptage, M.H. (1993). The inactivation of Fe-S cluster containing hydro-lyases by superoxide. J. Biol. Chem. *268*, 22369–22376.

Fridovich, I. (1970). Quantitative aspects of the production of superoxide anion radical by milk xanthine oxidase. J. Biol. Chem. *245*, 4053–4057.

Gardner, P.R., and Fridovich, I. (1991). Superoxide sensitivity of the *Escherichia coli* aconitase. J. Biol. Chem. *266*, 19328–19333.

Gardner, P.R., and Fridovich, I. (1992). Inactivation-reactivation of aconitase in *Escherichia coli*. A sensitive measure of superoxide radical. J. Biol. Chem. *267*, 8757–8763.

Gardner, P.R., Raineri, I., Epstein, L.B., and White, C.W. (1995). Superoxide radical and iron modulate aconitase activity in mammalian cells. J. Biol. Chem. *270*, 13399–13405.

Garthwaite, G., and Garthwaite, J. (1986). Neurotoxicity of excitatory amino acid receptor agonists in rat cerebellar slices: dependence on calcium concentration. Neurosci. Lett. *66*, 193–198.

Greenlund, L.J.S., Deckweth, T.L., and Johnson, E.M., Jr. (1995). Superoxide dismutase delays neuronal apoptosis: a role for reactive oxygen species in programmed neuronal death. Neuron *14*, 303–315.

Halliwell, B., and Gutteridge, J.M.C. (1989a). The chemistry of oxygen radicals and other oxygen-derived species. In Free Radicals in Biology and Medicine, B. Halliwell and J. M. C. Gutteridge, eds. (Oxford: Clarendon Press), pp. 22–85.

Halliwell, B., and Gutteridge, J.M.C. (1989b). Free radicals as a useful species. In Free Radicals in Biology and Medicine, B. Halliwell and J. M. C. Gutteridge, eds. (Oxford: Clarendon Press), pp. 366–416.

Hausladen, A., and Fridovich, I. (1994). Superoxide and peroxynitrite inactivate aconitase, but nitric oxide does not. J. Biol. Chem. *269*, 29405–29408.

Hewett, S.J., Csernansky, C.A., and Choi, D.W. (1994). Selective potentiation of NMDA-induced neuronal injury following induction of astrocytic iNOS. Neuron *13*, 487–494.

Hockenbery, D.M., Oltvai, Z.N., Yin, X.M., Milliman, C.L., and Korsmeyer, S.J. (1993). Bcl-2 functions in an antioxidant pathway to prevent apoptosis. Cell *75*, 241–251.

Jordan., Ghadge, G.D., Prehn, J.H.M., Toth, P.T., Roos, R.P., and Miller, R.J. (1995). Expression of human copper/zinc-superoxide dismutase inhibits the death of rat sympathetic neurons caused by withdrawal of nerve growth factor. Mol. Pharmacol. *47*, 1095–1100.

Kane, D.J., Sarafian, T.A., Anton, R., Hahn, H., Butler Gralla, E., Selverstrone Valentine, J., Ord, T., and Bredesen, D.E. (1993). Bcl-2 inhibition of neural death: decreased generation of reactive oxygen species. Science *262*, 1274–1277.

Kennedy, M.C., Emptage, M.H., Dreyer, J., and Beinert, H. (1983). The role of iron in the activation-inactivation of aconitase. J. Biol. Chem. *258*, 11098–11105.

Kinouchi, H., Epstein, C.J., Mizui, T., Carlson, E.J., Chen, S.F., and Chan, P.H. (1991). Attenuation of focal cerebral ischemic injury in transgenic mice overexpressing CuZn superoxide dismutase. Proc. Natl. Acad. Sci. USA *88*, 11158–11162.

Koh, J.Y., Goldberg, M.P., Hartley, D.M., and Choi, D.W. (1990). Non-NMDA receptor-mediated neurotoxicity in cortical culture. J. Neurosci. *10*, 693–705.

Krebs, H.A., and Holzach, O. (1952). The conversion of citrate into cis-aconitate and isocitrate in the presence of aconitase. Biochem. J. *52*, 527–528.

Lafon-Cazal, M., Pietri, S., Culcasi, M., and Bockaert, J. (1993). NMDA-dependent superoxide production and neurotoxicity. Nature *364*, 535–537.

Lerea, L.S., Butler, L.B., and McNamara, J.O. (1992). NMDA and non-NMDA receptor-mediated increase of c-fos mRNA in dentate gyrus neurons involves calcium influx via different routes. J. Neurosci. *12*, 2973–2981.

Liochev, S.I., and Fridovich, I.A. (1995). Cationic manganic porphyrin inhibits uptake of paraquat by *E. coli*. Arch. Biochem. Biophys. *321*, 271–275.

Lipton, S.A., Choi, Y.B., Pan, Z.-H., Lei, S.Z., Chen, H.V., Sucher, N.J., Loscalzo, J., Singel, D.J., and Stamler, J.S. (1993). A redox-based mechanism for the neuroprotective and neurodestructive effects of nitric oxide and related nitroso-compounds. Nature *364*, 626–632.

Monyer, H., Hartley, D.M., and Choi, D.W. (1990). 21-Aminosteroids attenuate excitotoxic neuronal injury in cortical cell cultures. Neuron *5*, 121–126.

McCord, J.M., and Fridovich, I. (1969). Superoxide dismutase: an enzymatic function for erythrocuprein (hemocuprein). J. Biol. Chem. *244*, 6049–6055.

Olney, J.W. (1986). Inciting excitotoxic cytocide among central neurons. In Advances in Experimental Medicine and Biology, Vol. 203, R. Schwarcz and Y. Ben-Ari, eds. (New York: Plenum Press), pp. 632–645.

Olney, J.W. (1989). Excitatory amino acids and neuropsychiatric diseases. Biol. Psychiatry *26*, 505–525.

Patel, M.N., Yim, G.K.W., and Isom, G.E. (1991). Blockade of N-methyl-D-aspartate receptors prevents cyanide-induced neuronal injury in primary hippocampal cultures. Toxicol. Appl. Pharmacol. *115*, 124–129.

Patel, M.N., Yim, G.K.W., and Isom, G.E. (1992). N-methyl-D-aspartate receptors mediate cyanide-induced cytotoxicity in hippocampal cultures. Neurotoxicology *14*, 35–40.

Puttfarcken, P.S., Getz, R.L., and Coyle, J.T. (1993). Kainic acid-induced lipid peroxidation: protection with butylated hydroxytoluene and U78517F in primary cultures of cerebellar granule cells. Brain Res. *624*, 223–232.

Rabizadeh, S., Gralla, E.B., Borchelt, D.R., Gwin, R., Valentine, J.S., Sisodia, S., Wong, P., Lee, M., Hahn, H., and Bredesen, D.E. (1995). Mutations associated with amytrophic lateral sclerosis convert superoxide dismutase from an antiapoptotic gene to a proapoptotic gene: studies in yeast and neural cells. Proc. Natl. Acad. Sci. USA *92*, 3024–3028.

Racker, E. (1950). Spectrophotometric measurements of the enzymatic formation of fumaric and cis-aconitic acids. Biochim. Biophys. Acta *4*, 211–214.

Reynolds, I.J., and Hastings, T.G. (1995). Glutamate induces the production of reactive oxygen species in cultured forebrain neurons following NMDA receptor activation. J. Neurosci. *15*, 3318–3327.

Rosen, D.R., Siddique, T., Patterson, D., Figlewicz, D.A., Sapp, P., Hentati, A., Donaldson, D., Goto, D., O'Regan, J.P., Deng, H.X., et al. (1993). Mutations in Cu/Zn superoxide dismutase gene are associated with familial amyotrophic lateral sclerosis. Nature *362*, 59–62.

Rothstein, J.D., Bristol, L.A., Hosler, B., Brown, R.H., Jr., and Kuncl, R.W. (1994). Chronic inhibition of superoxide dismutase produces apoptotic death of spinal neurons. Proc. Natl. Acad. Sci. USA *91*, 4155–4159.

Troy, C.M., and Shelanski, M.L. (1994). Down-regulation of copper/zinc superoxide dismutase causes apoptotic death in PC12 neuronal cells. Proc. Natl. Acad. Sci. USA *91*, 6384–6387.

Vassault, A. (1983). Lactate dehydrogenase. In Methods of Enzymatic Analysis, H. U. Bergmeyer, ed. (Weinheim: Verlag Chemie), pp. 118–126.